Differential force microscope for long time-scale biophysical measurements

Jason L. Choy[a],
Department of Chemistry, University of California at Berkeley, Berkeley, California 94720; UCSF/UC Berkeley Joint Graduate Group in Bioengineering, University of California at Berkeley, Berkeley, California 94720; and Graduate Group in Biophysics, University of California at Berkeley, Berkeley, California 94720

Sapun H. Parekh[a],
Department of Chemistry, University of California at Berkeley, Berkeley, California 94720; UCSF/UC Berkeley Joint Graduate Group in Bioengineering, University of California at Berkeley, Berkeley, California 94720; and Graduate Group in Biophysics, University of California at Berkeley, Berkeley, California 94720

Ovijit Chaudhuri,
Department of Chemistry, University of California at Berkeley, Berkeley, California 94720; UCSF/UC Berkeley Joint Graduate Group in Bioengineering, University of California at Berkeley, Berkeley, California 94720; and Graduate Group in Biophysics, University of California at Berkeley, Berkeley, California 94720

Allen P. Liu,
Department of Chemistry, University of California at Berkeley, Berkeley, California 94720; UCSF/UC Berkeley Joint Graduate Group in Bioengineering, University of California at Berkeley, Berkeley, California 94720; and Graduate Group in Biophysics, University of California at Berkeley, Berkeley, California 94720

Carlos Bustamante,
Department of Chemistry, University of California at Berkeley, Berkeley, California 94720; Department of Physics, University of California at Berkeley, Berkeley, California 94720; and Howard Hughes Medical Institute, University of California at Berkeley, Berkeley, California 94720

Matthew J. Footer,
Department of Biochemistry, Stanford University School of Medicine, Stanford, California 94305

Julie A. Theriot, and
Department of Biochemistry, Stanford University School of Medicine, Stanford, California 94305

Daniel A. Fletcher[b]
Department of Bioengineering, University of California at Berkeley, Berkeley, California 94720; UCSF/UC Berkeley Joint Graduate Group in Bioengineering, University of California at Berkeley, Berkeley, California 94720; and Graduate Group in Biophysics, University of California at Berkeley, Berkeley, California 94720

Abstract

[b]fletch@berkeley.edu.
[a]These authors contributed equally to this work.

Force microscopy techniques including optical trapping, magnetic tweezers, and atomic force microscopy (AFM) have facilitated quantification of forces and distances on the molecular scale. However, sensitivity and stability limitations have prevented the application of these techniques to biophysical systems that generate large forces over long times, such as actin filament networks. Growth of actin networks drives cellular shape change and generates nano-Newtons of force over time scales of minutes to hours, and consequently network growth properties have been difficult to study. Here, we present an AFM-based differential force microscope with integrated epifluorescence imaging in which two adjacent cantilevers on the same rigid support are used to provide increased measurement stability. We demonstrate 14 nm displacement control over measurement times of 3 hours and apply the instrument to quantify actin network growth *in vitro* under controlled loads. By measuring both network length and total network fluorescence simultaneously, we show that the average cross-sectional density of the growing network remains constant under static loads. The differential force microscope presented here provides a sensitive method for quantifying force and displacement with long time-scale stability that is useful for measurements of slow biophysical processes in whole cells or in reconstituted molecular systems *in vitro*.

INTRODUCTION

Cells possess an array of highly specialized protein machines that orchestrate and perform essential cellular functions such as division and motility. In recent years, force microscopy techniques including optical trapping, magnetic tweezers, and atomic force microscopy (AFM) have provided insight into the importance of physical forces and mechanical properties in the functioning of biological systems at the molecular level.[1]

A common limitation of these techniques is thermal drift of the probe (a bead the in case of optical and magnetic tweezers and a cantilever in the case of AFMs), as well as drift of the surrounding microscope components. If the drift rate is similar to the mechanochemical time scale for the biological system of interest, then it is impossible to obtain high fidelity force and position data. This limitation has recently been addressed for high-resolution tracking of molecular motors, such as RNA polymerase, through the use of a levitated optical trapping geometry.[2] Other attempts to reduce the influence of thermal effects include differential back focal plane detection for optical traps and differential cantilever or interferometric detection in single-molecule and imaging AFM applications.[3–6] However, these techniques have been demonstrated to probe systems that produce small forces over short times (approximately in seconds).

Here, we present the design and verification of an AFM-based differential force microscope that can achieve 14 nm absolute stability between the cantilever and surface for at least 3 hours. The instrument, which has recently been used in studies of actin network force generation and mechanics,[7,8] is integrated with an epifluorescence microscope and used here to obtain measurements showing that average network density (as measured by total fluorescence divided by network length) is constant under a fixed load.

ATOMIC FORCE MICROSCOPY FOR BIOPHYSICAL MEASUREMENTS

Coordinated multimolecule biological processes, such as actin polymerization, generate and respond to large forces over long times, and single-molecule force microscopy techniques are generally not appropriate for studying these processes. Actin filament networks, which generate protrusions during cell crawling and shape changes during phagocytosis, can generate nano-Newtons of force over time scales of minutes to hours through the addition of nanometer-scale actin monomers.[7,9] A study of their force generation capabilities has been

hindered by the lack of suitable techniques for probing them while at the same time imaging spatial and temporal changes in the organization of component proteins.

AFMs are attractive tools for investigating biophysical processes in cells like actin network growth since they are capable of measuring nanometer-scale displacements and a wide range of forces. Typical AFMs can measure forces well into the nano-Newton range, the scale of forces believed to be generated by actin-driven cellular processes such as pseudopod formation.[10] Furthermore, AFMs are easily integrated with fluorescence microscopes. In an ideal AFM force measurement, the position of the surface and the reference position of the cantilever are fixed in the laboratory frame, and changes in deflection of the cantilever's tip are equal to changes in the end-to-end distance of the sample under study and are related to the force exerted on the sample by Hooke's law.

In practice, however, drift caused by temperature fluctuations in the surrounding environment can cause spontaneous cantilever bending and unpredictable drift between the cantilever and surface. Cantilevers bend as temperature fluctuates, even in the absence of an externally applied force, which can result in a shift of the zero-force reference deflection of the cantilever.[11] Treatments such as thermal annealing, use of cantilevers without reflective or other asymmetric coatings, or torsional cantilevers can be used to reduce this effect.[11–13]

Over long times, temperature fluctuations and gradients can cause drift of the entire microscope apparatus, resulting in unwanted changes in the distance between the cantilever and surface that are much larger than cantilever bending and preclude accurate measurements of sample length.[4] Conventional AFM measurements with single cantilevers cannot distinguish between this cantilever-surface drift and actual sample length changes since both may result in cantilever deflection. Drift in commercial systems can exceed 20 nm/min, which is on the same order as actin network growth rates and can therefore mask changes in network length (data not shown). Cantilever-surface drift is a recognized limitation of AFM and has been addressed in a variety of ways for imaging, electrochemical, and single-molecule force spectroscopy applications.[4,6,14] Our differential force microscopy technique with integrated epifluorescence addresses cantilever-surface drift for molecular systems that generate large forces over long times.

INSTRUMENT DESIGN AND PERFORMANCE

Design principles

The instrument consists of an epifluorescence-equipped AFM modified to measure the deflection of two cantilevers simultaneously. In our system, two cantilevers—a "reference" and a "measurement" cantilever—attached to the same rigid support are mounted above a surface at a 10° angle (Fig. 1, inset) similar to the experimental geometry described previously in Altmann *et al.*[4] When undeflected (Fig. 1, inset gray dotted lines), the reference cantilever is closer to the surface than the undeflected measurement cantilever by a distance D_o and is the first to make contact when the surface is raised. If dS_r is the deflection of the reference cantilever when in contact with the surface and dS_m is the deflection of the measurement cantilever when in contact with the sample, the distance D between the tip of the measurement cantilever and the surface is

$$D(t) = D_o - dS_r(t) + dS_m(t). \tag{1}$$

Any drift in the position of the surface with respect to the measurement cantilever is detected by a change in dS_r. Feedback on dS_r or dS_m can be used to create three different modes of operation:

1. Drift clamp: Surface position is adjusted to keep dS_r constant, thus minimizing common-mode cantilever-surface drift from measurements of sample length and force over time.

2. Force clamp: Surface position is adjusted to keep dS_m constant, thus maintaining a constant force applied by the measurement cantilever over time, regardless of cantilever-surface drift. With dS_m fixed, changes in length are directly measured by changes in deflection of the reference cantilever (ΔdS_r).

3. Position clamp: Surface position is adjusted to keep ($dS_m - dS_r$) constant, thus maintaining a constant separation between the measurement cantilever and the surface over time, compensating for all cantilever-surface movement.

Optical lever detection

Deflections of the two cantilevers are monitored simultaneously with an objective-based optical lever system similar to that used by Wickramasinghe *et al.* and Schaffer and Hansma to monitor one cantilever[15] (Fig. 1, see the section on methods for a list of components). In our system, the cantilevers are positioned in the focal plane of a single infinity-corrected objective lens, and two independent lasers with different wavelengths are focused through the objective onto the two cantilevers. The beams reflected by the cantilevers are collected by the same objective and separated by a polarization-dependent beam splitter and dichroic mirrors onto two independent position sensitive photodetectors. Application of an external force to either cantilever causes that cantilever to bend, changing the angle of its reflecting surface. This change in angle is converted by the objective lens into a lateral shift in the position of the reflected beam on the position sensitive photodetector [Figs. 2(a) and 2(b)]. For a given change in cantilever angle α, the angle of the reflected beam with respect to the optical axis changes by 2α. The corresponding shift in the position Δh of the beam on the detector can then be expressed as

$$\Delta h = f[\tan(\theta) - \tan(\theta + 2\alpha)], \tag{2}$$

where f is the focal length of the objective lens and θ is the angle of incidence of the laser on the cantilever relative to the optical axis. The bending angle of the cantilever can further be related to the displacement of the cantilever's tip, y, using the relation

$$\alpha = \tan^{-1}(3y/2l), \tag{3}$$

where l is the length of the cantilever.[16] The sensitivity of this detection scheme is similar to that of traditional optical lever designs as demonstrated by the instrument's ability to resolve thermally limited deflections of the cantilever during cantilever calibration [Fig. 2(c)].[17,18]

The use of an objective lens to both focus the incident beams and collect the reflected beams provides several advantages over a free-space design for monitoring two cantilevers and an interferometer-optical lever combination.[4,5] First, the lasers share a beam path over much of their trajectories, simplifying the optical path and enabling additional lasers to be added with minimal perturbation. Second, our system is compatible with smaller cantilevers that offer improved force resolution.[19] An objective lens with a higher numerical aperture could be

used to focus the lasers more tightly onto the reduced dimensions of the small cantilevers. Finally, use of an objective lens enables reflection and transmission imaging (Fig. 1) of the cantilevers and sample for easy alignment. We note that this instrument is designed to measure sample displacement and force and is not intended for topographical imaging applications in its current form.

Spatial stability characterization

As a demonstration of the utility of our differential force microscope, we measured its ability to control cantilever-surface separation over long times. This was done by monitoring how the distance between the measurement cantilever and the surface changed with time immediately after the cantilevers were immersed in a standard biological buffer. We compared the cantilever-surface drift when the instrument was operated as a position clamp to when no differential feedback was used (Fig. 3). During the test, the measurement cantilever was freely suspended above the surface, and the reference cantilever was held in contact to monitor the surface position. At regular intervals, cantilever-surface separation was measured by bringing the surface into contact with the measurement cantilever.

When the position clamp (feedback) was active [Fig. 3(a), inset], the root-mean-square (rms) deviation in the cantilever-surface separation with respect to the initial value was fewer than 14 nm over 3 hours [$n = 8$, Fig. 3(a)] and showed no clear time dependence. This is in sharp contrast to the results obtained when the clamp was not used where position error accumulated with time and was often more than 2000 nm at the end of a measurement [$n = 8$, Fig. 3(b)]. This two order of magnitude reduction in drift demonstrates the ability of our AFM-based differential force microscope to dramatically minimize unwanted cantilever-surface drift for long time-scale experiments. While these results illustrate the advantage of this differential AFM technique, we note that even better performance may be obtained by using two cantilevers with the same physical dimensions and adjusting the angle of the sample surface to impose an asymmetry in the cantilever-surface distance between the cantilevers. In principle, this approach could reduce the differential cantilever drift, which may be responsible for the residual 14 nm error in our spatial stability measurements with the position clamp active.

APPLICATION TO ACTIN NETWORK GROWTH

As an application of this instrument to probe force-generating biophysical systems, we used the differential force microscope in the force-clamp mode to monitor actin network growth between the measurement cantilever and surface. We detected changes in the actin network length with the reference cantilever and held a force of 36 nN on the network with the measurement cantilever (Fig. 4, upper inset). Actin network growth was localized to the measurement cantilever by nonspecifically adsorbing the bacterial nucleation promoting factor, ActA, directly onto the measurement cantilever's surface (see the section on methods). No ActA was adsorbed onto the reference cantilever. Both cantilevers were then immersed in *Xenopus laevis* cytoplasmic extract, in which ActA activates the Arp2/3 complex to stimulate the growth of a branched actin filament network.[7,20]

A low concentration of rhodamine-actin was added to the extract and incorporated into the network, allowing network growth to be visualized through the integrated epifluorescence microscope. Cantilever deflection was recorded continuously while fluorescence images were taken at 10 min intervals to quantify the amount of polymerized actin at the cantilever's surface (Fig. 4, lower inset). The measured network length was found to directly correlate with increasing fluorescence intensity (Fig. 4, solid line and crosses). The ratio of fluorescence intensity to length varied little over the experiment with a standard deviation less than 2.7% of the mean, demonstrating that the average cross-sectional network density

did not change noticeably as the network elongated under a constant force. This finding suggests that network density is independent of extrinsic variables such as network length and depends solely on opposing force, which sheds light onto the dynamics of the actin cytoskeleton in motile cells experiencing stable loading conditions. This combination of length, force, and fluorescence measurement capabilities provides a platform for quantifying how average network density changes as a function of force and as a function of time when the network is subjected to various loading conditions.

DISCUSSION AND CONCLUSIONS

The instrument presented here employs a differential cantilever geometry in which two cantilevers on a single substrate were used to stabilize AFM measurements of force and distance. The stabilization geometry we describe is conceptually similar to that used in Altmann *et al.*,[4] though we measure beam-bounce deflection through a single objective lens that can be used for simultaneous imaging and alignment of the cantilevers. Furthermore, our instrument is targeted at biological processes that operate over significantly longer times (at larger forces) than the ~10 s stability necessary for force spectroscopy measurements of protein unfolding.[4] In the stability demonstrations from Altmann *et al.* the authors utilize a feedback loop in which the reference cantilever alone provides the feedback signal for drift stabilization over short time scales, which neglects spontaneous differential cantilever drift between the two cantilever sensors over longer time scales. We show that both sources of drift can be addressed by employing a position clamp using differential feedback, achieving two orders of magnitude improvement in precision over the case without differential feedback. To our knowledge, this is the first direct demonstration of drift control between the cantilever substrate and surface over time scales of several hours.

In summary, we have developed an AFM-based differential force microscope for probing coordinated, time-dependent multimolecule systems with a position stability of 14 nm over 3 hours. In the case of actin network growth, this stability corresponds to measurement uncertainty of less than four actin monomers. The ability to measure precise displacements combined with simultaneous time-lapse fluorescence imaging and existing strategies for the localization of molecules to the cantilever make this instrument useful for measuring mechanical and spatial biophysical changes in multimolecule systems over long times.[21] In addition to the actin network growth measurements that we present here, the differential force microscope could be used to quantify forces and nanometer-scale displacement during other cellular processes such as filopodia extension, phagocytosis, cytokinesis, and mitotic spindle formation.

METHODS

Differential force microscope components

An optical schematic of the the differential force microscope is shown in Fig. 1. The entire microscope is constructed horizontally on an optical breadboard housed in an acoustic enclosure (Technical Manufacturing Corporation) and vibrationally isolated with pneumatic support (Newport, Inc.). The main components in the schematic are the lasers, $\lambda 1$ (λ=670 nm, Point Source, Ltd.) and $\lambda 2$ (λ=635 nm, Thorlabs, Inc.), the closed-loop Z-axis piezoelectric stage (range=12 μm, accuracy=0.05 nm, Physik Instrumente, LP), commercial cantilevers (Veeco Metrology, Inc.), position sensitive detectors (PSDs) (Pacific Silicon Sensors, Inc.), and the objectives, OBJ1 (Mitutoyo 10×, 0.28 numerical aperture) and OBJ2 (Zeiss, 32×, 0.4 numerical aperture). All other components were purchased from standard optics suppliers (Thorlabs, Inc. and Edmund Optics, Inc.) or custom made. The entire instrument is controlled with custom written software in LABVIEW (National Instruments, Inc.)

Protein preparation

Actin was purified from rabbit skeletal muscle,[22] labeled on random lysines with NHS-rhodamine (Pierce Biotechnology, Inc.) and cycled repeatedly to ensure polymerization competency. *Xenopus laevis* extract was prepared, as previously described.[23] Following isolation, crude extract was ultracentrifuged for clarification, aliquoted, and stored at −80 °C. Extract mix was prepared by diluting the extract to 50% with *Xenopus* buffer (100 mM KCl, 0.1 mM $CaCl_2$, 2 mM $MgCl_2$, 5 mM EGTA, and 10 mM HEPES pH 7.7), spin filtering through 100 nm pores (Millipore) to remove large particulates, and adding 37.5 μl of 50% extract to 1.7 μl of energy mix (150 mM creating phosphate, 2 mM EGTA, 20 mM $MgCl_2$, and 20 mM ATP pH 7.4) and 2 μl of rhodamine-actin (2 mg/ml).

Actin network force-clamp measurements

The measurement cantilever had a stiffness of 20 pN/nm, and the reference cantilever had a stiffness of 30 pN/nm based on the manufacturer value and confirmed with thermal noise measurements [Fig. 2(c)].[18] The cantilever was functionalized by dipping the end into a solution of ActA (0.4 mg/ml) for 30 s, placed in a fluid cell, and immersed in *Xenopus laevis* extract after the surface was moved within ~100 μm of the cantilevers. Subsequently, cantilever deflection was calibrated, and the surface was finely adjusted with the piezoelectric stage until the desired force was reached on the measurement cantilever, after which data acquisition, force-feedback, and time-lapse fluorescence microscopy commenced. Data were antialiased at 50 Hz (Krohnhite, Inc.), recorded at 100 Hz using a PCI-6036E data acquisition board (National Instruments, Inc.), used for real-time software feedback, and saved for offline processing in IGOR PRO 5 (Wavemetrics, Inc.).

Acknowledgments

References

1. Bustamante C, Chemla VR, Forde NR, Izhaky D. Annu Rev Biochem. 2004; 73:705. [PubMed: 15189157]

2. Shaevitz JW, Abbondanzieri EA, Landick R, Block SM. Nature (London). 2003; 426:684. [PubMed: 14634670]

3. Nugent-Glandorf L, Perkins TT. Opt Lett. 2004; 29:2611. [PubMed: 15552661]

4. Altmann SM, Lenne PF, Horber JKH. Rev Sci Instrum. 2001; 72:142.

5. Sparks AW, Manalis SR. Nanotechnology. 2006; 17:1574.Appl Phys Lett. 2004; 85:3929.

6. Schitter G, Stemmer A. Nanotechnology. 2002; 13:663.

7. Parekh SH, Chaudhuri O, Theriot JA, Fletcher DA. Nat Cell Biol. 2005; 7:1119.

8. Chaudhuri O, Parekh SH, Fletcher DA. Nature (London). 2007; 445:295. [PubMed: 17230186]

9. Marcy Y, Prost J, Carlier MF, Sykes C. Proc Natl Acad Sci USA. 2004; 101:5992. [PubMed: 15079054]

10. Vonna L, Wiedemann A, Aepfelbacher M, Sackmann E. J Cell Sci. 2003; 116:785. [PubMed: 12571276]

11. Radmacher M, Cleveland JP, Hansma PK. Scanning. 1995; 17:117.

12. Savran CA, Burg TP, Fritz J, Manalis SR. Appl Phys Lett. 2003; 83:1659.

13. Beyder A, Spagnoli C, Sachs F. Rev Sci Instrum. 2006; 77

14. Abraham DW, Williams CC, Wickramasinghe HK. Appl Phys Lett. 1988; 53:1503.Tabard-Cossa V, Godin M, Beaulieu LY, Grutter P. Sens Actuators B. 2005; 107:233.

15. Wickramasinghe HK. J Vac Sci Technol A. 1990; 8:363.Schaffer TE, Hansma PK. J Appl Phys. 1998; 84:4661.

16. Sarid, D. Scanning Force Microscopy: With Applications to Electric, Magnetic, and Atomic Forces. Oxford University Press; New York: 1994.

17. Meyer G, Amer NM. Appl Phys Lett. 1988; 53:1045.Drake B, et al. Science. 1989; 243(4898): 1586. [PubMed: 2928794]

18. Hutter JL, Bechhoefer J. Rev Sci Instrum. 1993; 64:1868.

19. Viani MB, Schaffer TE, Chand A, Eiwd M, Gaub HE, Hansma PK. J Appl Phys. 1999; 86:2258.Walters DA, Cleveland JP, Thomson NH, Hansma PK, Wendman MA, Gurley G, Elings V. Rev Sci Instrum. 1996; 67:3583.

20. Cameron LA, Giardini PA, Soo FS, Theriot JA. Nat Rev Mol Cell Biol. 2000; 1:110. [PubMed: 11253363]

21. Gimzewski JK, Joachim C. Science. 1999; 283:1683. [PubMed: 10073926] Weizmann Y, Patolsky F, Lioubashevski O, Willner J. J Am Chem Soc. 2004; 126:1073. [PubMed: 14746475] Wu GH, et al. Proc Natl Acad Sci USA. 2001; 98:1560. [PubMed: 11171990]

22. Spudich JA, Watt S. J Biol Chem. 1971; 246:4866. [PubMed: 4254541]

23. Cameron LA, Footer MJ, van Oudenaarden A, Theriot JA. Proc Natl Acad Sci USA. 1999; 96:4908. [PubMed: 10220392]
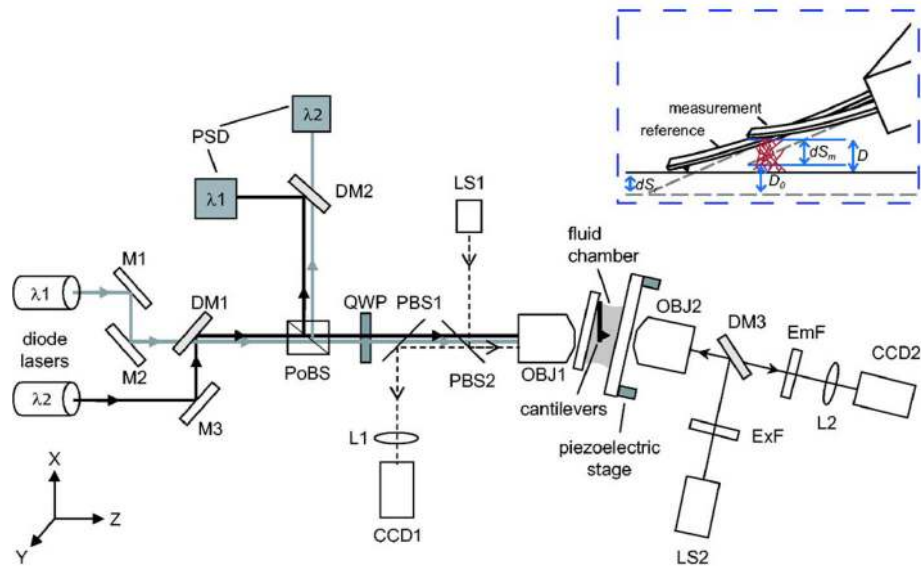
FIG. 1.
(Color online) Optical schematic of the differential force microscope. Two similarly polarized diode lasers ($\lambda 1$ and $\lambda 2$) are steered by mirrors (M1, M2, M3), combined by a dichroic mirror (DM1), and focused through a microscope objective (OBJ1) onto the two cantilevers. The reflected beams are collected by the same objective, reflected by a polarization beam splitter (PoBS), and separated by a dichroic mirror (DM2) onto two position sensitive detectors (PSDs). The cantilevers and sample can be illuminated with a broadband light emitting diode source (LS1) via a pellicle beams splitter (PBS2) and OBJ1, enabling both reflection (OBJ1, PBS1, L1, CCD1) and transmission (OBJ2, L2, CCD2) imaging. Epifluorescence imaging of the sample (OBJ2, L2, CCD2) is obtained by fluorescence illumination with a mercury arc lamp (LS2) via OBJ2 through an excitation-emission cube (ExF, DM3, EmF). A feedback-controlled piezoelectric stage is used to control surface position. (Inset) Diagram showing the two-cantilever geometry of the differential AFM technique and drift correction principle. Actin network (red lines) length (D) can be accurately quantified over long times without the influence of cantilever-sample drift by monitoring deflection of a measurement (dS_m) and reference cantilever (dS_r) simultaneously. Because the reference cantilever is in contact with the surface at all times, any common-mode cantilever-surface movement will be directly quantified as a change in dS_r, making it possible to eliminate this error from measurements of actin network growth. Dotted lines (gray) depict the original position of the surface position and undeflected cantilevers.
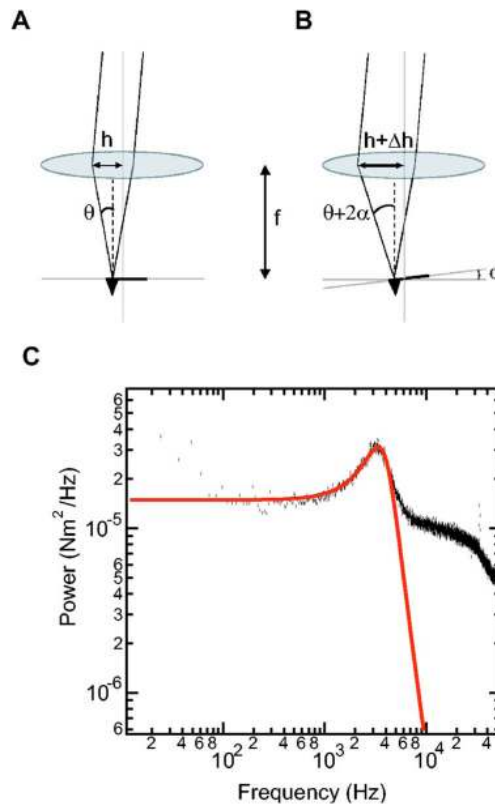
FIG. 2.
(Color online) Ray optics diagram of the objective-based optical lever and power spectrum
of cantilever noise, both shown for a single cantilever. (A) Light incident on the undeflected
cantilever reflects at an angle θ and is displaced from the optical axis upon reflection by a
distance $h = f \tan(\theta)$ at the principal plane of the objective (shown here as a single lens). (B)
Upon bending, the cantilever reflecting surface changes by an angle α, shifting the angle of
the reflected beam by an amount of 2α and changing the lateral displacement of the beam at
the principal plane of the objective to $h = f \tan(\theta + 2\alpha)$. Thus, the cantilever bending angle α
is detected as a lateral displacement $\Delta h = f[\tan(\theta) - \tan(\theta + 2\alpha)]$. (C) Power spectrum of a
freely suspended cantilever in *Xenopus* buffer (see section on methods). The first resonance
of the raw power spectrum (black dots) is fit with a Lorentzian function (red line), which is
characteristic of a damped, driven harmonic oscillator, demonstrating that our differential
AFM setup is thermally limited. Data were acquired at 100 kHz and antialiased to 50 kHz.
Spring constants were extrapolated from the fitted power spectra using the equipartition
theorem and were in the range of 29–33 pN/nm, which is within 20% of the manufacturer's
value of 30 pN/nm (Ref. 18).
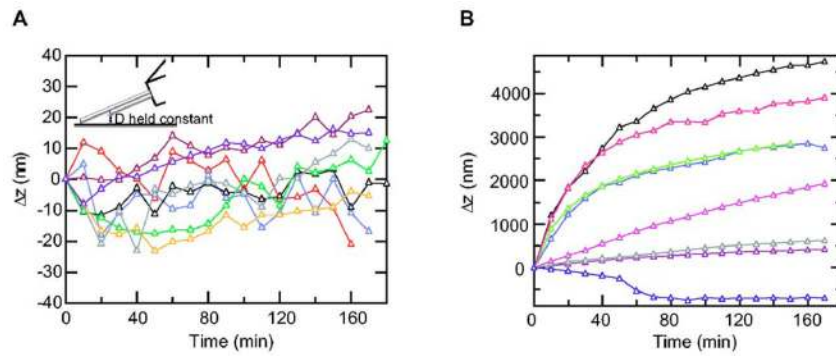
FIG. 3.
(Color online) Cantilever-surface drift, Δz, with position clamp active. In all experiments, data acquisition (100 Hz) was initiated 2–4 min after the cantilevers were immersed in *Xenopus* buffer, and the measurement cantilever was freely suspended while the reference cantilever was held in contact with the surface. To quantify the drift, the cantilever-surface separation was sampled at 10 min intervals by moving the surface into contact with the measurement cantilever. Individual data points (open triangles in both panels) are connected with line segments, and different colors indicate different experiments. (A) Graph showing Δz vs time for position clamp experiments where differential feedback was used to keep cantilever-surface separation, D, constant (inset). The rms Δz was always less than 14 nm over an individual 3 h measurement period, and the absolute Δz never exceeded 22 nm (n =8). (B) Experiments where the position clamp was inactive showed an absolute Δz often greater than 2000 nm after 3 h (n =8).
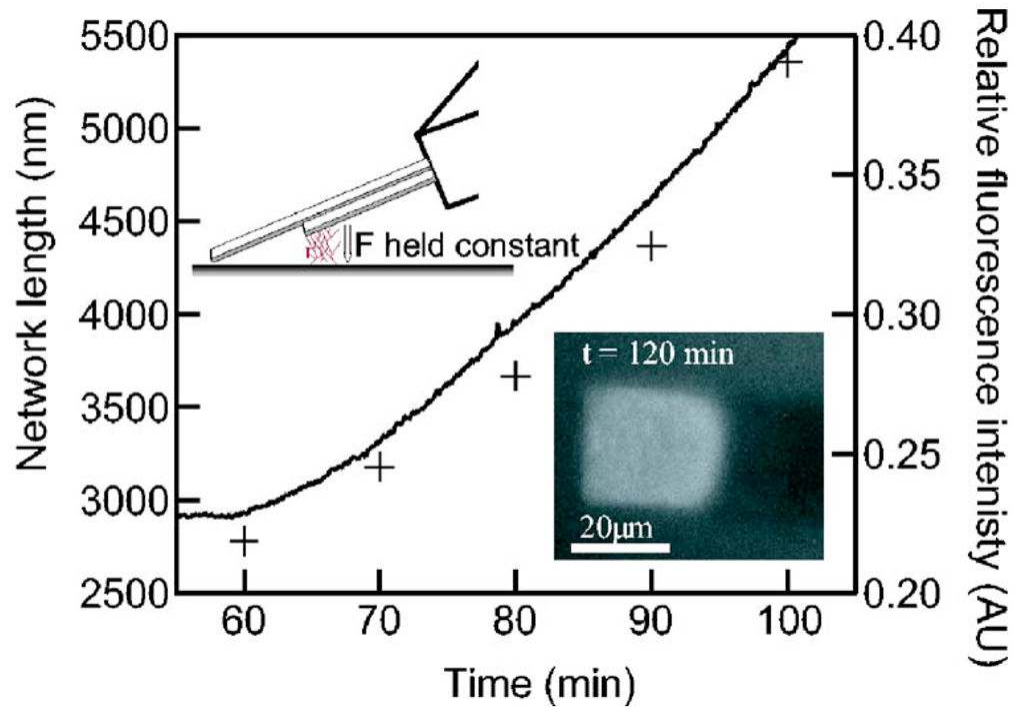
FIG. 4.
(Color online) Simultaneous force and fluorescence microscopy of actin network growth in a force clamp. Length vs time (solid line) plot of actin network growth under a constant force $F =36$ nN applied by the measurement cantilever (upper inset). Length changes were measured continuously by the reference cantilever, and fluorescence images of rhodamine-actin (lower inset) in the network were taken at 10 min intervals. Relative fluorescence intensity (crosses) directly correlated with network length as the network elongated, indicating that the average cross-sectional density of the network did not change as the network grew against the applied force. Data acquistion and fluorescence imaging were started 2–4 min after cantilevers were immersed in extract mix.